論文 / 著書情報
Article / Book Information

論題(和文)	RESPONSE ESTIMATION WITH LIMITED SENSORS VIA EQUIVALENT-INPUT DISTURBANCE METHOD
Title(English)	
著者(和文)	鄭湧臻, 陳引力, 佐藤大樹, 宮本皓, 佘錦華
Authors(English)	Zheng Yongzhen, Yinli Chen, Daiki Sato, Kou Miyamoto, Jinhua She
出典 / Citation	日本建築学会関東支部研究報告集， I， ，pp. 313-316
Citation(English)	， I， ，pp. 313-316
発行日 / Pub. date	2026，3
権利情報	一般社団法人 日本建築学会

RESPONSE ESTIMATION WITH LIMITED SENSORS VIA EQUIVALENT-INPUT DISTURBANCE METHOD

構造－振動

正会員 ○ 鄭湧臻 *1　正会員 陳引力 *1
〃 佐藤大樹 *1　〃 宮本皓 *2
〃 佘錦華 *3

Equivalent-Input Disturbance　Disturbance estimation　State estimation
Sensor-limited structures　Observer design　Base-isolated building

1. Introduction

Structural health monitoring and active control systems increasingly rely on real-time responses of a building. However, in practical engineering applications, installing sensors on every floor is rarely feasible due to cost, accessibility, and maintenance constraints[1]. This limitation motivates the need for accurate state estimation methods capable of reconstructing structural responses from a limited number of measured signals.

She *et al*, proposed the equivalent-input disturbance (EID) approach to reject the disturbance induced response[2]. Miyamoto *et al*. extended the EID approach to the active structural control and disturbance estimation[3]. However, previous studies did not consider the response estimation of the system.

The objective of this study is to propose a new method to estimate the responses of the system using EID-based approach. A numerical example using a 100-m high-rise base-isolated building with limited sensors to validate the effectiveness of the proposed method. From the numerical example, we confirmed that the proposed method has a relatively high estimation accuracy compared with the conventional observer.

2. Mathematic model

The dynamics of a multiple degree-of-freedom (DOF) system subjected to ground motion is

$$M_s\ddot{x}(t) + C_s\dot{x}(t) + K_s x(t) = -M_s\mathbf{1^n}\ddot{x}_g(t) \tag{1}$$

where $x(t)$ is the displacement vector, M_s, C_s, and K_s are the mass, damping, and stiffness matrices, respectively, $\ddot{x}_g(t)$ is the ground acceleration, and $\mathbf{1^n}$ is the all-ones vector.

The state-space representation of (1) is

$$\begin{cases} \dot{z}(t) = Az(t) + B_g\ddot{x}_g(t) \\ y(t) = Cz(t) \end{cases} \tag{2}$$

in which

$$z(t) = \begin{bmatrix} x(t) \\ \dot{x}(t) \end{bmatrix} \tag{3}$$

$$A = \begin{bmatrix} \mathbf{0^{n\times n}} & \boldsymbol{I^{n\times n}} \\ -M_s^{-1}K_s & -M_s^{-1}C_s \end{bmatrix} \tag{4}$$

$$B_g = \begin{bmatrix} \mathbf{0^n} \\ \mathbf{-1^n} \end{bmatrix} \tag{5}$$

where $z(t)$ is the state vector, $y(t)$ is the output of the system, A is the system matrix, and the input matrix B_g is the input gain of $\ddot{x}_g$, C is the output matrix.

3. Design of EID estimator

This report uses EID approach[3] to estimate all states of the system. The block diagram is shown in Fig. 1. In Fig. 1, $\hat{z}$ is the estimated state, $\hat{y}$ is the estimated output, and $\hat{\ddot{x}}_g$ is the estimated seismic excitation.

The state observer gain L is designed by linear quadratic regulator (LQR) using the following performance index:

$$J = \int_0^\infty [\Delta z(t)^T Q \Delta z(t) + u^T(t) R u(t)]\mathrm{d}t \tag{6}$$

$$\Delta z(t) = z(t) - \hat{z}(t) \tag{7}$$

where Q is the weighting matrix for $\Delta z(t)$, R is the weighting matrix for $u(t)$, The definition of $u(t)$ is

$$u(t) = L^T \Delta z(t) \tag{8}$$

Upon solving the optimal problem of (6), the observer gain L is

$$L = PC^T R^{-1} \tag{9}$$

where $P = P^T \geq 0$ is the solution of the following algebraic Riccati equation:

$$AP + PA^T - PC^T R^{-1} CP + Q = 0 \tag{10}$$

Also, in Fig. 1 an EID estimator is incorporated to estimate the seismic input and apply it to the observer to reduce the estimation error of the system.

In Fig. 1, B_g^+ is a pseudo-inverse of B_g and is given by the following equation[2]:

$$B_g^+ = \frac{B_g^T}{B_g^T B_g} \tag{11}$$

Furthermore, a low pass filter, $F(s)$, is used to remove high-frequency noise. This study uses the following first-order low-pass filter:

$$F(s) = \frac{N_F}{T_F s + 1} \tag{12}$$

where N_F is the filter gain, T_F is cut-off period of the filter and s is the Laplace operator.

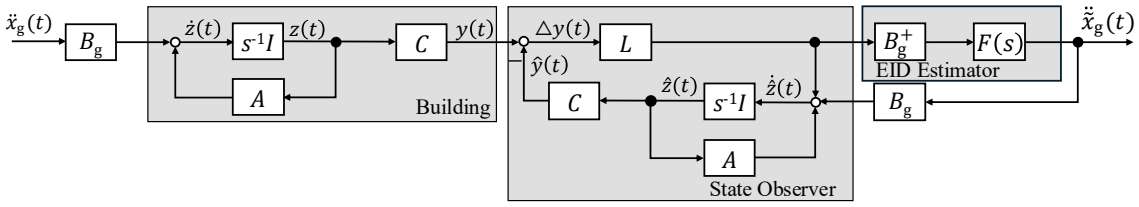

Figure 1. Block diagram of system.

4. Numerical example

This study uses a high-rise base-isolated building model with a total of 100-m height (Fig. 2(a)). The building is modeled as a 25 DOFs shear-building model (Fig. 2(b)). Tables 1 and 2 shows the parameters of the superstructure and base-isolated story, respectively.

Table.1 Parameter of superstructure.

Parameter	Symbol	Valve
Height	H	100 m
Height of each story	H_i	4 m
Width	B	25 m
Depth	D	25 m
Density	ρ	200 kg/m^3
DOF	-	25
1st natural period	T	2 s
1st damping ratio	h	0.01

Table.2 Parameter of base-isolated story.

Parameter	Symbol	Valve
Width	B_0	25 m
Depth	D_0	25 m
Mass per unit area	ρ_0	3000 kg/m^3
DOF	-	1
Isolated period	T_0	4 s
Isolated damping ratio	h_0	0.20

Thus, the definitions of $x(t)$, M_s, C_s, and K_s in (1) are

$$x(t) = [x_0(t)\ x_1(t)\ \cdots\ x_{25}(t)]^T \tag{13}$$

$$M_s = \begin{bmatrix} m_0 & & & & \\ & m_1 & & & \\ & & \ddots & & \\ & & & m_{24} & \\ & & & & m_{25} \end{bmatrix} \tag{14}$$

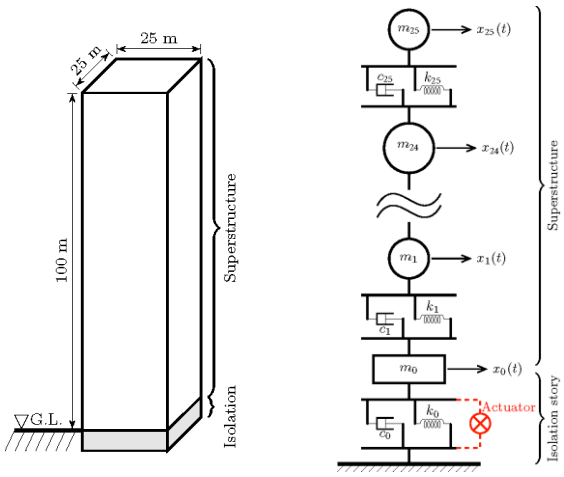

(a) Building (b) Model

Figure 2. Building and mathematic model.

$$K_s = \begin{bmatrix} k_0 + k_1 & -k_1 & & & \\ -k_1 & k_1 + k_2 & -k_2 & & \\ & -k_2 & \ddots & \ddots & \\ & & \ddots & k_{24} + k_{25} & -k_{25} \\ & & & -k_{25} & k_{25} \end{bmatrix} \tag{15}$$

$$C_s = \begin{bmatrix} c_0 + c_1 & -c_1 & & & \\ -c_1 & c_1 + c_2 & -c_2 & & \\ & -c_2 & \ddots & \ddots & \\ & & \ddots & c_{24} + c_{25} & -c_{25} \\ & & & -c_{25} & c_{25} \end{bmatrix} \tag{16}$$

in this model, x_i represents the displacement of the i^{th} story; m_i, k_i and c_i are the mass, stiffness coefficient and damping coefficients of the i^{th} story, respectively. Note that $i = 0$ represents the isolation layer. The calculation of k_i follows the method proposed by Sato *et al*[4]. m_i and c_i are defined as

$$m_i = \rho BDH_i \tag{17}$$

$$c_i = \frac{hT}{\pi} k_i \tag{18}$$

In this study, the acceleration sensors are installed on the BIS-story, 5th story, 10th story, 15th story, 20th story, 25th story, and the displacement sensor is only installed on the BIS-story.

Thus, C, C_{OD}, C_{OA}, and C_A are defined as follows:

$$C = \begin{bmatrix} C_{\mathrm{OD}} \\ C_{\mathrm{OA}} C_{\mathrm{A}} \end{bmatrix} \tag{19}$$

$$C_{\mathrm{OD}} = [1 \quad 0 \quad 0 \quad \cdots \quad 0]_{1\times 26} \tag{20}$$

$$C_{\mathrm{OA}} = [e_1^{\mathrm{T}} \quad e_6^{\mathrm{T}} \quad e_{11}^{\mathrm{T}} \quad e_{16}^{\mathrm{T}} \quad e_{21}^{\mathrm{T}} \quad e_{26}^{\mathrm{T}}]^{\mathrm{T}} \tag{21}$$

$$C_{\mathrm{A}} = [-M_{\mathrm{s}}^{-1}K_{\mathrm{s}} \quad -M_{\mathrm{s}}^{-1}C_{\mathrm{s}}] \tag{22}$$

in which,

$$e_k = [\overbrace{0 \quad \cdots \quad 0}^{k-1} \quad 1 \quad \overbrace{0 \quad \cdots \quad 0}^{26-k}]_{1\times 26} \tag{23}$$

where C_{OD} and C_{OA} are the matrix representing locations of sensors of displacement and acceleration, respectively, C_{A} is the acceleration-output matrix.

The weighting matrices for designing the observer gain and the parameters low-pass filter are given below:

$$Q = \begin{bmatrix} 10^{-10} I_{26} & 0 \\ 0 & 10^{15} I_{26} \end{bmatrix} \tag{24}$$

$$R = 1 \tag{25}$$

$$N_{\mathrm{F}} = 22 \tag{26}$$

$$T_{\mathrm{F}} = 0.01 \tag{27}$$

The input ground motion used in this study is a code earthquake motion, with a pseudo velocity-response spectrum (p*S*v) of 100 cm/s (damping ratio = 5%). And phase characteristics are based on the Hachinohe 1968 NS[5].

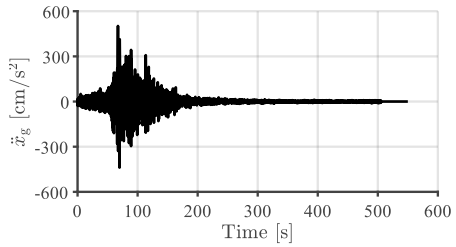

Figure 3. Time-history wave of Code Hachinohe.

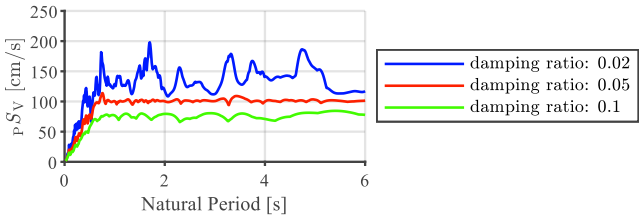

Figure 4 Pseudo velocity-response spectrum of Code Hachinohe.

We compare two different cases:

Case 1: A system contains only a state observer without the EID estimator (see Fig. 5).

Case 2: A system contains a state observer and EID estimator. The EID signal is subjected to the state observer (proposed method, see Fig. 1).

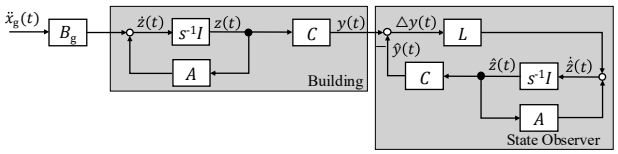

Figure 5. Block diagram of case 1.

5. Simulation Results

Fig. 6 illustrates the comparison of the estimated and the original input wave. From Fig. 6, earthquake wave simulated by the EID consistently exhibits great agreement with the original earthquake wave.

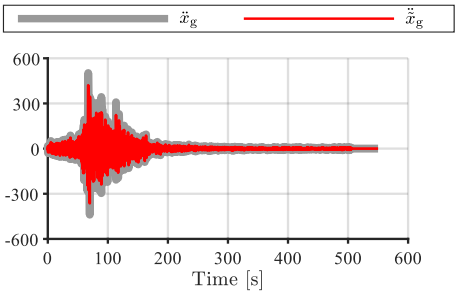

Figure 6. Estimation of input wave: original wave vs. estimated wave

Fig. 7 presents a comparison of the maximum response of each floor under seismic excitation among the actual structural responses (building), the observer with EID (case 2), and the observer without EID (case 1).

(1) Displacement and inter-story drift

Fig. 7(a) and 7(d) indicate that the displacement responses are accurately estimated for all cases.

(2) Velocity and acceleration

For velocity and acceleration estimation, the observer without EID exhibits noticeable estimation errors. In contrast, the proposed method shows significantly improved estimation accuracy.

Fig. 8 shows the comparation of the time-history waves of actual structural responses and cases 1-2. From Fig. 8, it can be confirmed that the time-history waves of the proposed method are in close agreement with those of the actual building.

6. Conclusion

This paper presented a response estimation approach based on the EID method for buildings with limited number of sensors. Simulation results show that the proposed method achieves high estimation accuracy.

References

1) El-Qawasma, F.A., Elfouly, T.M. and Ahmed, M.H.: Minimising Number of Sensors in Wireless Sensor Networks for Structure Health Monitoring Systems, IET Wirel. Sens. Syst., Vol.9, pp. 94-101, 2019.4

2) J. She, M. Fang, Y. Ohyama, H. Hashimoto and M. Wu.: Improving Disturbance-Rejection Performance Based on an Equivalent-Input-Disturbance Approach, IEEE Transactions on Industrial Electronics, Vol.55, no.1, pp. 380-389, 2008.

3) K. Miyamoto, J. She and D. Sato: Active Structural Control with Suppression of Absolute Acceleration Using Equivalent-Input-Disturbance Approach, IEEE 27th International Symposium on Industrial Electronics (ISIE), Cairns, QLD, Australia, pp. 1089-1093, 2018
4) D. Sato, K. Kasai, and T. Tamura: Influence of Frequency Sensitivity of Viscoelastic Damper on Wind-Induced Response [in Japanese], Journal of Structural and Construction Engineering (Transactions of AIJ), vol.74, no.635, pp. 75-82, 2009
5) 翠川三郎，三浦弘之: 1968 年十勝沖地震の八戸港湾での強震記録の再数値化，日本地震工学会論文集, vol.10, no.2, pp.12-21, 2010

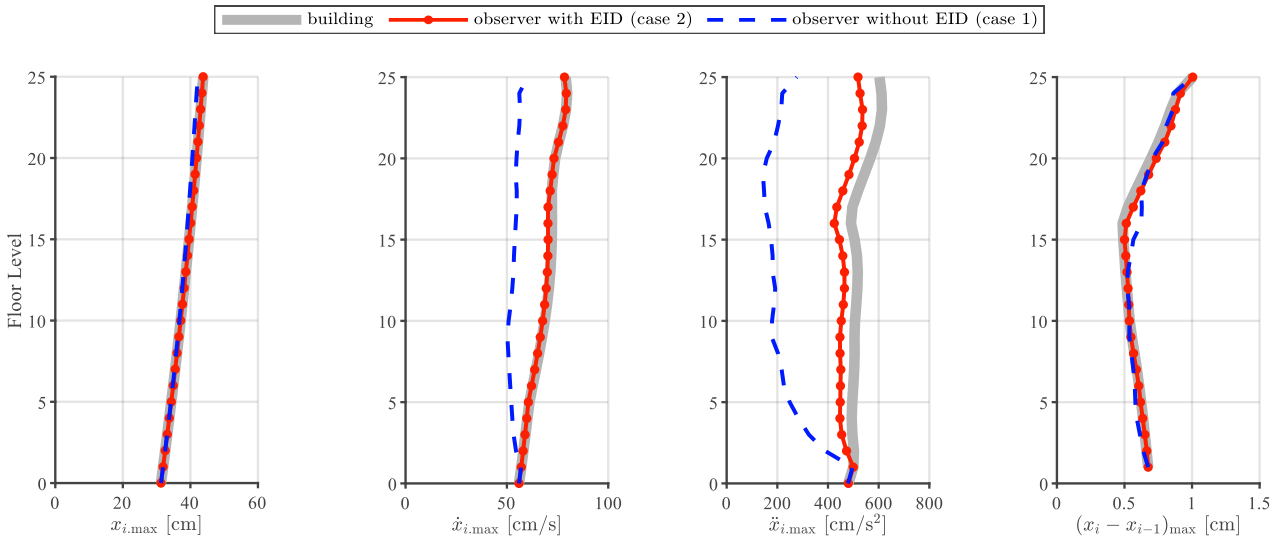

(a) Displacement (b) Velocity (c) Acceleration (d) Inter-story drift

Figure 7. Max responses of each story (building vs. observer with and without EID).

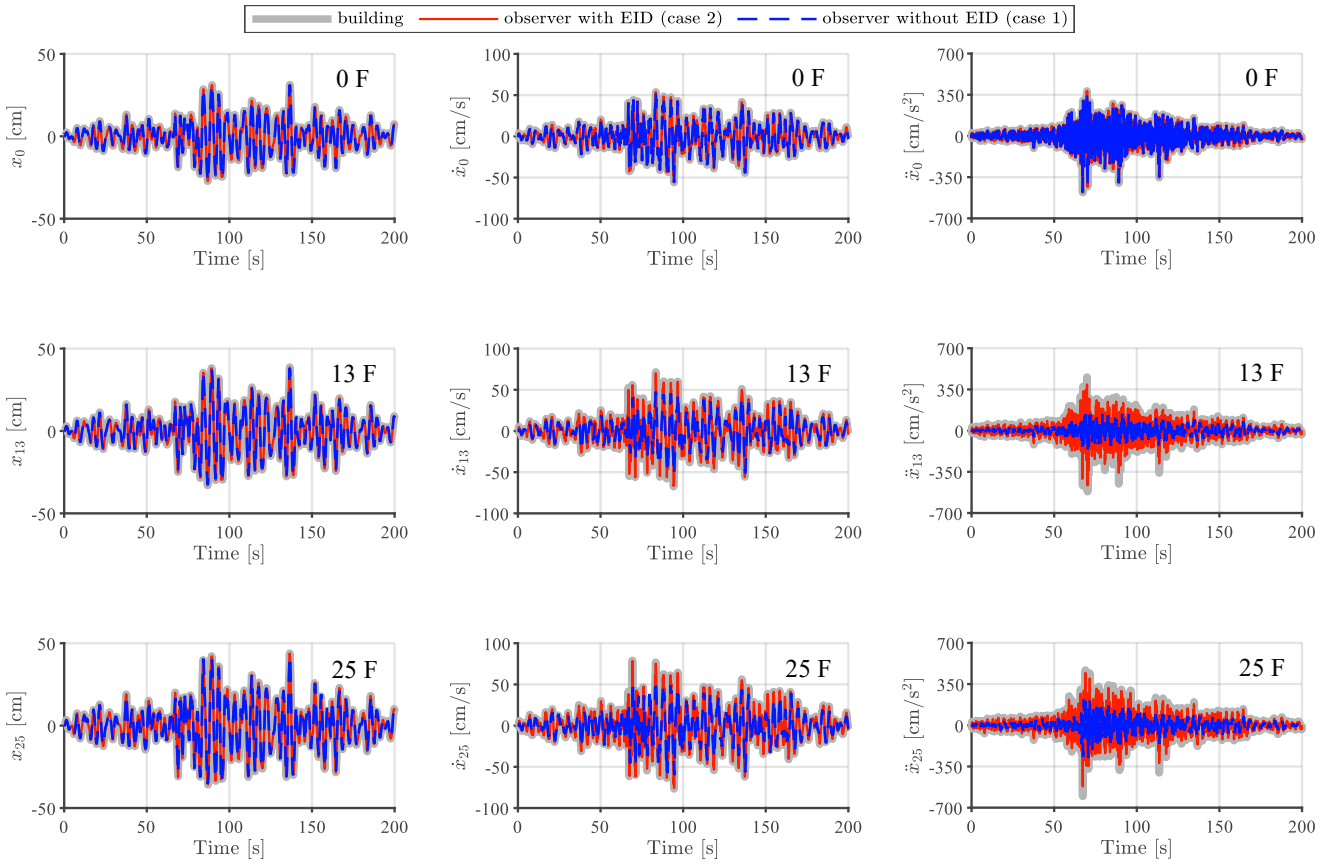

(a) Displacement (b) Velocity (c) Acceleration

Figure 8. Time history waves of base-isolated, middle and top layer.

＊1 東京科学大学 Institute of Science Tokyo
＊2 清水建設 Shimizu corporation
＊3 東京工科大学 Tokyo University of Technology